

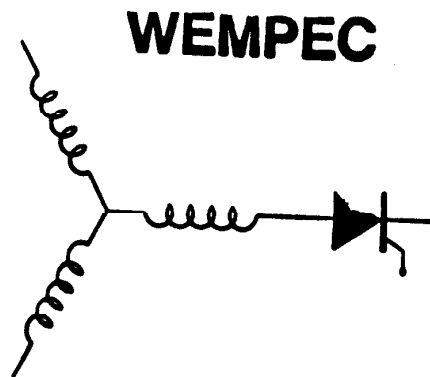
Wisconsin Electric Machines and Power Electronics Consortium

RESEARCH REPORT
90-19

Utilization of the Series Resonant DC Link as a DC Motor Drive

P. Caldeira, K.W. Marschke
M.T. Aydemir, T.A. Lipo
Dept. of Electrical & Computer Eng.
University of Wisconsin - Madison
1415 Johnson Drive
Madison, Wisconsin 53706, USA

Y. Murai
Dept. of Electronics & Computer Eng.
Gifu University
1 - 1 Yanagido
Gifu, Gifu 501-11, Japan



Department of Electrical and Computer Engineering
1415 Johnson Drive
Madison, Wisconsin 53706

Utilization of the Series Resonant DC Link as a DC Motor Drive

P. Caldeira, K. W. Marschke,
M. T. Aydemir, T. A. Lipo
Dept. of Electrical & Computer Eng.
University of Wisconsin-Madison
1415 Johnson Drive
Madison, WI 53706, USA

Y. Murai
Dept. of Electronics & Computer Eng.
Gifu University
1-1 Yanagido
Gifu, Gifu 501-11, Japan

Abstract

In this paper a high frequency series resonant dc link converter is utilized as a dc motor drive. This system generates a resonant current in a series link and switching is done at zero current instants, reducing switching losses to a minimal value. A Pulse Density Modulation (PDM) strategy, utilizing a current regulator loop and an external motor speed feedback loop, controls the resonant converter. A sinusoidal input fundamental current and nearly unity input power factor can be observed in different load conditions. The overall characteristics of the system, including such variables as maximum power, input current, start up, and transient responses are presented by digital simulation and verified on an actual prototype system.

Introduction

High power converters can be broadly classified accordingly to their switching modes as:

- a) hard switching
- b) soft switching

In a hard switching converter type, semiconductor devices are switched with high values of current or voltage, while in a soft switching type the switching of the devices is made at zero voltage or zero current instants. Soft switched converters not only have high power density but also possess very low switching losses. High power density ac/ac converters utilizing resonant link schemes with the purpose to soft switch the high speed semiconductor devices, have recently been developed.

In general, switching schemes for resonant converters can be classified according to their resonant ac link and resonant dc link modes of operation. The resonant ac circuits utilize a parallel or series resonant link, impressing both polarities of ac voltage and current on the link thus requiring bidirectional switches in the input and output converters [1-3]. The resonant dc circuits can also utilize a parallel or series resonant link. The majority of resonant dc link converters reported in the past have been restricted to parallel resonant types [4-5].

The series dc link circuits realize pulsating dc currents in the link by adding dc offsets to the ac resonant currents. A high frequency series resonant dc link, ac-to-ac power converter is proposed in [6] utilizing only 12 unidirectional switches and is the dual of the parallel resonant dc link system [4]. As shown in Fig. 1,

the capacitor C_0 and inductor L_0 cause a resonant high frequency current i_s to flow from the input ac source to the load while the inductance L_d provides dc bias, I_d , to the resonant current i_s . This current then becomes unidirectional allowing the utilization of high power thyristors as the switching element. Four thyristors conducting in series in two bridges turn on and off at zero current instants, reducing switching losses significantly. In [6] proportional and derivative current loop feedback and a damping series R-C circuit were utilized to minimize current pulse fluctuation and system instability of the proposed resonant system. Introduction of losses and load dependency are disadvantages of this solution.

A current pulse control strategy for this high frequency resonant scheme is proposed in [7]. Through adequate regulation of the current delivered to the load the output voltage error can be minimized. A circulating thyristor TCRC, is utilized to avoid overexcitation of capacitors C_0 and C_L .

Different dc drive controls, such as phase control, integral cycle control, and chopper control [8], are well known methods for obtaining a controllable dc voltage from a dc or ac source. In phase control the input voltage is applied to the dc motor during intervals of each half-cycle, while in the integral mode different number of half-cycles are applied to the motor during a certain period. In the chopper control mode, with or without the rectification stage, the control of the amplitude of the output voltage is obtained varying the duration of the on cycle of the switches [9].

Single and three phase thyristor phase-controlled converter circuits utilized as a dc motor drive can be classified as half-wave, semi-converter, full-converter or dual-converter (where two full-converters are connected in parallel), offering 1, 2 or 4 quadrant operation in the voltage and current plane. Switching losses, due to the hard switching process, high ripple frequency (varying from the supply frequency, f_s , to $6f_s$) limited control of the input power factor and harmonic content, can be cited as disadvantages of the existing systems.

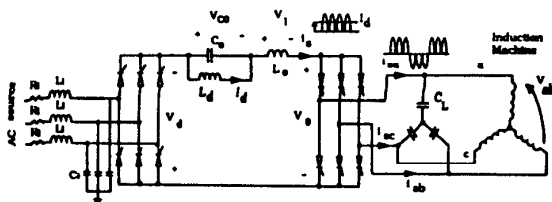


Fig. 1 AC/AC drive system utilizing the series resonant link

Series Resonant Link Converter as a DC Motor Drive

The series resonant link converter is an extremely versatile power conversion system and can be utilized in many applications such as a power conditioning system for SMES [10]. In this application the transfer of energy into a large inductive coil L_d is accomplished through the regulation of the DC current I_d in this coil. This paper proposes the use of the series resonant dc current link converter as a DC motor drive. The DC motor armature is placed in series with the bias inductor L_d , as shown in Figure 2. As in the SMES application the current ripple frequency is approximately the resonant frequency. Consequently the size of the series inductor can be reduced to obtain acceptable torque ripple.

The high resonant frequency is determined by the resonant elements L_0 and C_0 . The switching frequency is always slightly lower than the resonant frequency due to the additional time needed to reach the required forward voltage over the switch to maintain stability.

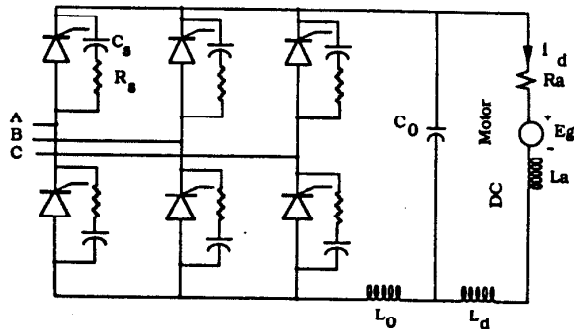


Fig. 2 Series resonant dc link converter utilized as a dc motor drive

A very efficient system is then obtainable with operation at high frequencies with reduced switching losses, since the switching losses are nearly eliminated by the soft switching of the semiconductor devices. The resonant pulse constitutes the control unit and since high resonant frequencies can be obtained (20 to 35 kHz) the resonant pulses can be distributed in the input phases through many forms of Pulse Density Modulation (PDM) corresponding to the system requirements such as low harmonic content, complete control of the input power factor including the distortion and displacement factors. Consequently, nearly sinusoidal fundamental input current can be obtained, with improved harmonic content when compared with hard-switching schemes. Since the output voltage of the resonant converter can be reversed, the system is fully regenerative.

The complete control strategy and overall performance obtained through digital simulation, for start-up, steady state, and under load variation utilizing a separately excited DC motor are presented in this paper. Experimental results for different control strategies are also presented.

Monophase Model

In [11] a monophase model was utilized for the analytical analysis of the resonant DC current link utilized as ac/ac drive system. Figure 3 shows the monophase model for the resonant dc current link used as a dc motor drive system. The following equations and initial conditions can be derived from Figure 3:

$$-V_d + v_c(t) + v_l(t) + v_{sw}(t) = 0 \quad (1)$$

$$v_c(t) = \frac{1}{C_0} \int_0^t i_0(t) dt = \frac{1}{C_0} \int_0^t (i_s(t) - I_d) dt \quad (2)$$

$$v_l(t) = L_0 \frac{di_s}{dt} \quad (3)$$

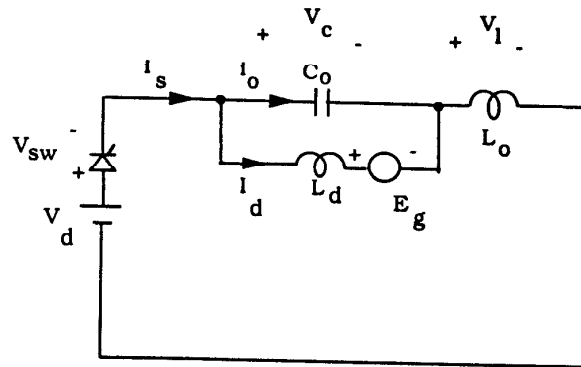


Fig. 3 Monophase model of the resonant current link ac/dc drive system

$$v_c(0) = V_{c0} \quad i_s(0) = 0. \quad (4)$$

The solution of these differential equations is

$$i_s(t) = I_d - I_d \cos \omega_0 t + \left(\frac{V_{swt}}{Z_0} \right) \sin \omega_0 t \quad (5)$$

$$v_c(t) = (V_d) - I_d Z_0 \sin \omega_0 t - V_{swt} \cos \omega_0 t \quad (6)$$

where

$$Z_0 = \sqrt{\frac{L_0}{C_0}} \quad \omega_0 = \frac{1}{\sqrt{L_0 C_0}} \quad V_{swt} = V_d - V_{c0}. \quad (7)$$

V_{c0} represents the initial voltage over the resonant capacitor at the beginning of the current pulse. The voltage V_{swt} is the required forward bias across the switching element, guarantying a minimum turn-off time and stable operation under different load conditions.

Figure 4 shows the resonant current $i_s(t)$, voltage over the resonant capacitor and inductor, $v_c(t)$ and $v_l(t)$ respectively, and voltage over the switches $v_{sw}(t)$ for different resonant cycle conditions, that is for positive and negative values of the excitation

voltage, V_d . During the turn-off process a negative voltage is applied over the switches with a minimum peak value equal to $V_{swt} + E_g$ (where E_g is the emf of the dc motor). This reverse voltage increases the speed of the turn-off process by increasing the carrier extraction from the cathode-anode junction of the semiconductor devices. Moreover the presence of this negative voltage allows the utilization of SCR's as main switches, instead of GTO's, if the device speed is compatible with the resonant frequency desired.

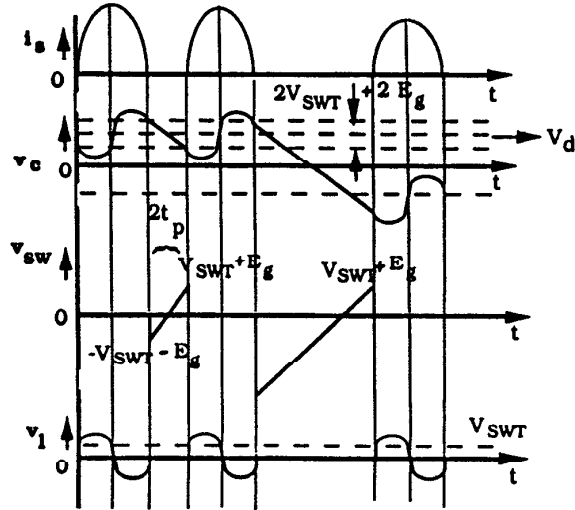


Fig. 4 Resonant current, resonant capacitor voltage, voltage over the switches and resonant inductor voltage in the monophase model

Control Strategy

The complete control of the converter and dc machine is shown in Fig. 5. For the control of the resonant converter, it can be observed that the average value of the resonant pulses is approximately the value of the dc motor current (I_d bias current). Through an adequate switching sequence of the input converter regulation of I_d is obtained. If large variations in I_d occurs the current pulses i_s will not reach zero any more, which would not allow the intended zero current switching procedure for this type of system or even causing hard-switching. A current regulator for the dc motor is then a mandatory condition. The dc motor current is compared with a reference value and an error signal is generated, which is transformed in a three-phase current signal. These current references are then compared with the actual input currents and three error signals are generated (e_a, e_b, e_c). As the sum of these errors must satisfy the relation

$$e_a + e_b + e_c = 0 \quad (8)$$

all of them can not have the same polarity. Hence, the triggering principle can be established as,

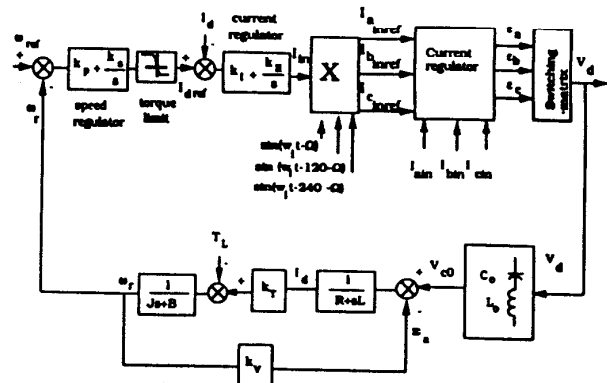


Fig. 5 Speed control for a dc motor drive system

- the thyristor in the phase having the larger error out of the two phases of the same polarity is chosen to be triggered
- the phase corresponding to the error with the opposite polarity error is selected as the other triggering phase.

Speed (ω) and current (I_d) of the dc motor are measured and compared with reference quantities (ω_{ref} and I_{dref}) in the speed and current loops respectively. The error generated in the motor speed loop goes through a proportional-integral regulator and generates a current reference signal (I_{dref}) which is compared with the motor current I_d . The following equations are valid for a dc motor and its control:

$$E_g = K_V \omega_r \quad (9)$$

$$T_e = K_T I_d \quad (10)$$

$$T_e = J \frac{d\omega_r}{dt} + B\omega_r + T_L \quad (11)$$

$$\omega_r = -\frac{K_T I_d - T_L}{J_s + B} \quad (12)$$

where ω_r represents the motor speed, B is the viscous damping coefficient, J is the total rotor inertia, E_g is the motor back emf, and K_T and K_V are torque and emf constants.

Simulation Results

A dc motor with the following parameters has been utilized as load for the resonant converter utilized as a dc motor drive:

Rated power : 10HP

$L_s = 4.3$ mH

$R_s = 0.57 \Omega$

$J = 0.0881$ kgm/rad/sec²

$B = 0.02$ kgm/rad/sec

$T_{rated} = 40.65$ Nm

$\omega_{rated} = 1750$ rpm = 183.26 rad/sec

Figure 6 shows the motor current, motor voltage and three-phase bridge input current and voltage in steady state operation of the dc motor driven by the resonant converter with a load torque of 35 Nm. Figure 7 shows the harmonic content of the input current during steady-state operation. Figure 8 and 9 show the variation of the motor current when the load torque varies from 35 Nm to 10 Nm and to a no load condition respectively. As can be noticed, the control distributes the resonant pulses in the input phases in a attempt to keep sinusoidal input fundamental current in phase with the input voltage in a wide range of operational load conditions.

The motor can be maintained at a constant speed during different transient conditions, such as changes in the load torque. With a no load operation, the motor speed initially increases, returning slowly to the its reference value (ω_{ref}) due to the effect

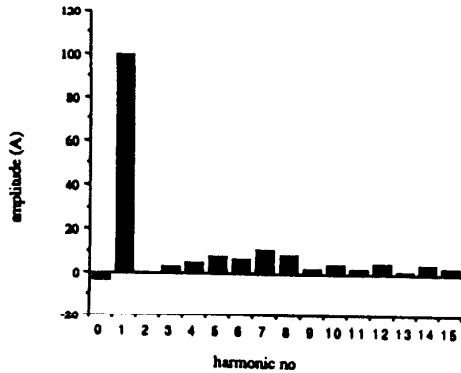


Fig. 7 Harmonic content of the input current under steady state operation

of the friction of the machine (B). The motor current, I_d , has then a very small value in this circumstance and discontinuous operation is reached. When the load is reduced to zero, the dc motor speed increases, above the reference value. A negative value for the reference current is generated. Since the motor has a small friction coefficient (B), its speed returns slowly to the reference value, and continuous operation is again obtained.

During motor current variation (both increase and decrease

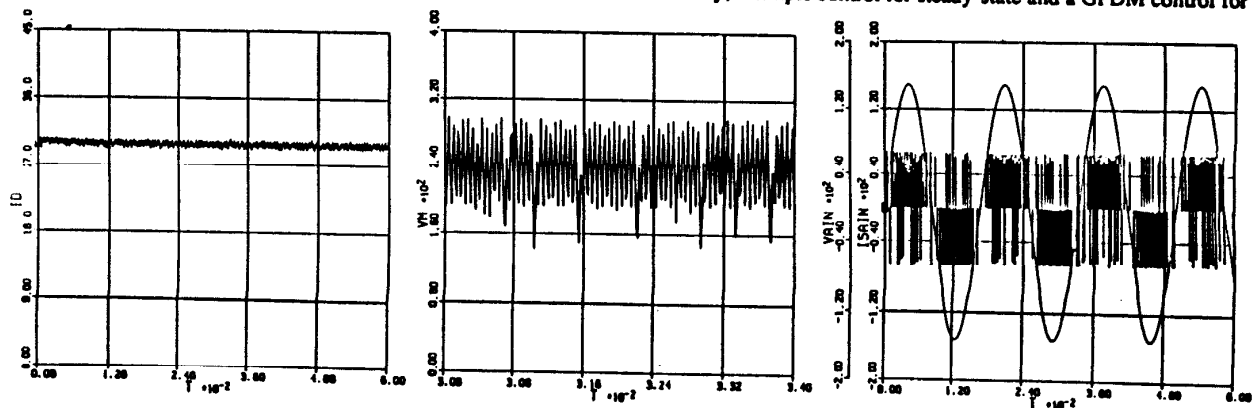


Fig. 6 Motor current, voltage and input current and voltage in steady state for a load torque of 35 Nm

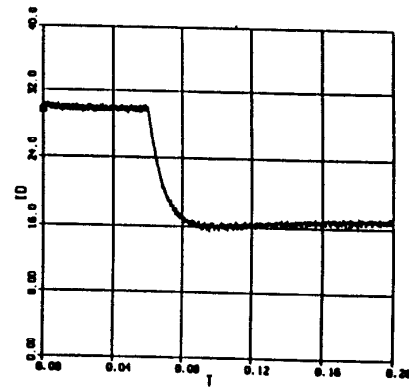


Fig. 8 Motor current under load torque variation (35 Nm to 10 Nm)

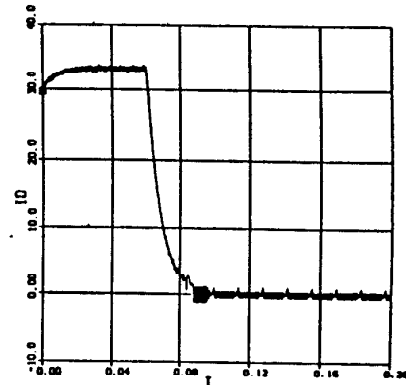


Fig. 9 Motor current under load torque variation (35 Nm to no load)

of the load torque), an improved harmonic content and input power factor can be obtained if the resonant pulses are placed in the conducting phases in a rate accordingly to the input voltages amplitude. Geometric Pulse Density Modulation can then be utilized in the periods of load variation. Figure 10 presents the simulated input current and its harmonic content during a transient period. In this way, a simple control for steady-state and a GPDM control for

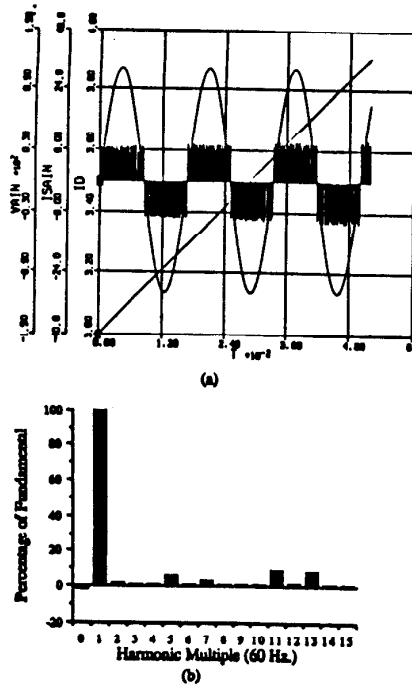


Fig. 10 Input current, input voltage, motor current and its spectrum during load variation, demonstrating the Geometric Pulse Density Modulation technique

transient operation, allow a continuous control of the input power factor, including input current distortion and displacement factors.

Converter Performance

Figures 11 shows the variation of power factor, displacement factor and harmonic factor with respect to the motor speed, for the resonant dc link converter utilized as a dc motor drive. Three different curves are presented in each case, for motor load torque of 35 Nm, 20 Nm and 10 Nm, with a smoothing reactor of 30mH. The input power factor curve shows an improved result in relation to conventional dc motor drive system, since its dependency

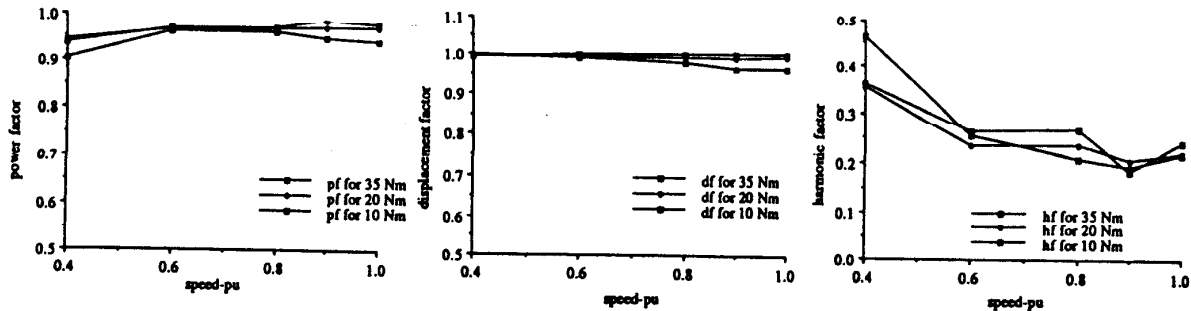


Fig. 11 Power factor, displacement factor and harmonic factor for the resonant dc motor drive

of the firing angle has been eliminated in the resonant scheme. Values of 0.9 and above were obtained for the input power factor for a large speed range. The displacement factor is approximately 1 for all speed ranges, since that was one of the main objectives of the implemented control. The harmonic factor presents again a better performance than conventional dc drive system. For a speed range above 0.35 pu, its value is below 0.4.

Figure 12 demonstrates the effect of the variation of the series inductor (L_d) in the peak current values of the motor current. As the series inductor value decreases, the ripple in the motor current increases. As can be observed, for a 10HP dc motor drive a series inductance of 5 mH gives reasonable ripple factor.

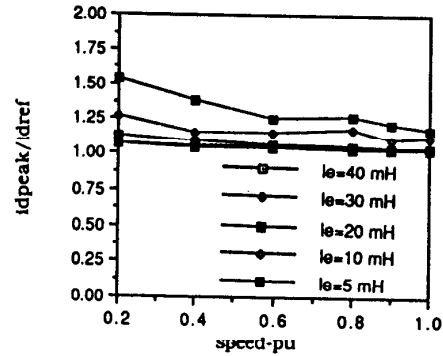


Fig. 12 Variation of ripple factor with respect to the motor speed for different values of the smoothing inductor ($T_L = 35$ Nm)

Alternative Resonant Topology

In an attempt to reduce losses over the resonant inductor L_0 , an alternative topology, shown in Fig. 13, can be utilized where the resonant inductor is in parallel with the bias inductor and dc motor. In this configuration the current I_d does not circulate through the inductor L_0 during the duration of the resonant pulse. Similar waveforms were obtained for the motor current, voltage and input current in the alternative resonant topology.

The conventional resonant topology presents a better power factor at higher speed while the alternative topology has a better power factor at low speed. At light loads both topologies have the same power factor. Both topologies have very good displacement factor at different load condition and speed. At higher speeds the

alternative resonant topology demonstrates a better harmonic factor than the conventional resonant topology. At heavy loads, the alternative resonant topology has a better ripple factor, while at light loads the conventional resonant topology presented a better ripple performance. The alternative resonant topology has a better overall performance for smaller values of the external inductance (L_d) if compared with the conventional resonant one.

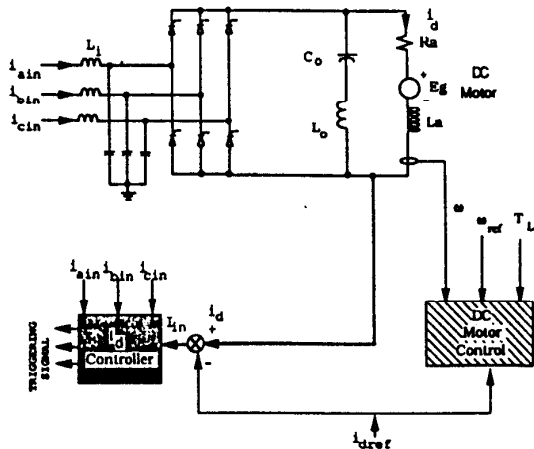


Fig. 13 Alternative topology for the resonant drive system

Device utilization

Different devices have been proposed to be utilized with this system, like GTO's in the gate assisted turn-off mode with a series fast recovery diode and an anti-parallel diode, with the purpose of decreasing the necessary turn-off time. Resonant frequencies of the order of 32kHz were reached in the experimental model. Since the resonant pulses reaches zero naturally, SCR's constitute an ideal choice for the resonant converter switches. Resonant frequencies of 27kHz were obtained in the model if the device is kept at room temperature. An increase in the device's temperature requires a large turn-off time, which can cause failures in the switching process.

Considering that the switching losses are extremely reduced, operations at low temperature (80°F) should be possible, allowing sufficient turn-off time for the device. Resonant peak currents of 120A, and I_d currents of 45 A with a turn-off time varying from 3 to 5 μ s were obtained for the SCR in the experimental system. Switches known as Zero Turn-off Thyristors (ZTO) constitute an ideal switch for this application, considering that the turn-off time requirement for these devices is extremely reduced.

Dual Converter

If operational conditions requires that the dc motor operates in forward and reverse direction, a mechanical contactor could be utilized to invert the armature polarity. Considering the volume of the arc extinction chamber and the losses introduced by the contactor, two resonant converters in opposite directions connected

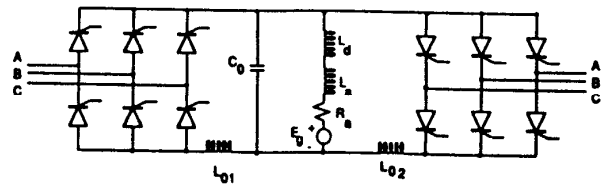


Fig. 14 Dual resonant converter dc motor drive

in parallel can be utilized for this purpose, allowing the flow of the motor current in any desired direction. With this topology four-quadrant operation is obtained. Figure 14 shows the resonant converter in a dual-converter topology.

Experimental Results

Figure 15 shows the three-phase experimental model assembled in the laboratory. An input ac voltage of 115Vac was utilized. Gate assisted turn-off thyristors with a series diode and anti-parallel diode were utilized as the main switching devices. The resonant converter components are:

- $L_0 = 60 \mu\text{H}$
- $C_0 = 0.3 \mu\text{F}$
- $L_d = 45 \text{ mH}$

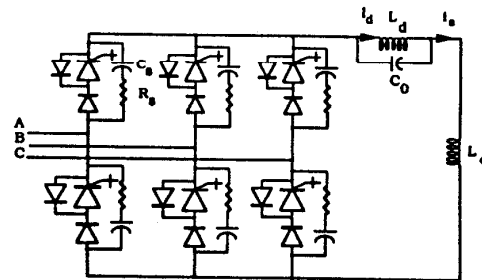


Fig. 15 Three phase experimental prototype for the resonant converter

Figure 16 shows the bias current I_d at a resonant frequency of 32kHz, that would circulate through the machine in the resonant dc motor drive .

Figure 17 shows the variation of I_d current , input current and voltage during a transient acceleration period. As can be notice the resonant pulses are distributed in the input lines in ratios correspondents to the input voltage amplitude (Geometric Pulse Density Modulation). Fig 18 shows the controlled variation of the current I_d . Through the utilization of positive and negative energy pulses, obtained from positive and negative values of the output bridge voltage V_d respectively, the acceleration and deceleration time of the dc motor can be fully controlled.

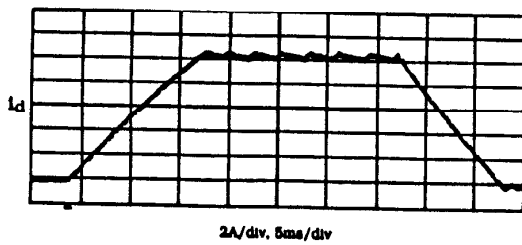
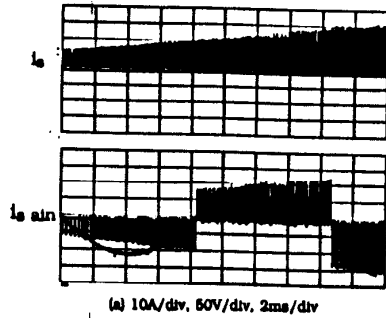
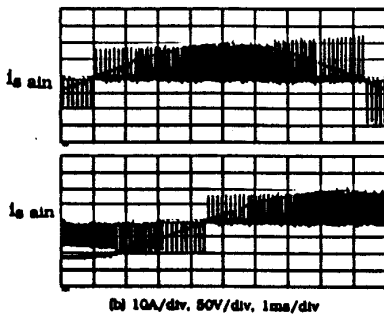


Fig. 16 DC motor current I_d

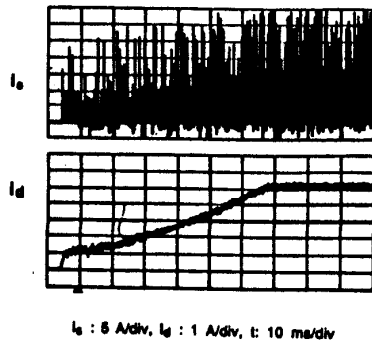


(a) 10A/div, 50V/div, 2ms/div



(b) 10A/div, 50V/div, 1ms/div

Fig. 17 Resonant current, resonant voltage and input current demonstrating the GPDM control ability during transient periods



$I_e : 8 \text{ A/div}, I_d : 1 \text{ A/div}, t : 10 \text{ ms/div}$

Fig. 18 Controlled variation of the dc motor current

References

- [1] P. Sood and T. A. Lipo, "Power Conversion Distribution System Using a Resonant High-Frequency AC Link", IEEE-IAS Annual Meeting Conference Record, pp. 533-541, 1986.
- [2] H. K. Lauw, J. B. Klaassens, N. G. Butler and D. B. Seely, "Variable-Speed Generation with the Series-Resonant Converter", IEEE-PES Winter Meeting Conference Record, 1987/1988.
- [3] S. W. H. de Haan and J. D. Lodder, "A Formalistic Approach to Series-Resonant Power Conversion", EPE Conference Record, pp. 231-238, 1987.
- [4] D. M. Divan, "The Resonant DC Link Converter--A New Concept in Static Power Conversion", IEEE IAS Annual Meeting Conference Record, pp. 648-656, 1986.
- [5] D. M. Divan and G. L. Skibinski, "Zero Switching Loss Inverters for High Power Applications", IEEE IAS Annual Meeting Conference Record, pp. 627-634, 1987.
- [6] Y. Murai and T. A. Lipo, "High Frequency Series Resonant DC Link Power Conversion", IEEE IAS Annual Meeting Conference Record, pp. 772-779, 1988.
- [7] Y. Murai, S. Mochizuki, P. Caldeira, T. A. Lipo, "Current Pulse Control of High Frequency Series Resonant DC Link Power Converter", Conf. Rec. of the 1989 IEEE-IAS Annual Meeting, pp. 1023-1030, 1989.
- [8] P. C. Sen, "Thyristor DC Drives", John Wiley & Sons, Inc., 1981.
- [9] P. C. Sen and M.L. MacDonald, "Thyristorized DC Drives with Regenerative Braking and Speed Reversal", IEEE Transactions on Industrial Electronics and Control Instrumentation, Vol. IECI-25, No.4, November 1978.
- [10] K. W. Marschke, P. Caldeira and T. A. Lipo, "Utilization of the Series Resonant DC Link as a Conditioning System for SMES", IEEE PESC Conference Records, pp. 266-271, 1990.
- [11] Caldeira P., Lipo T. A., Y. Murai, S. Mochizuki, "Design and Control of a Resonant DC Current Link AC/AC Drive System", IPEC Conference Records, pp. 397-404, 1990.